Miniaturized system for isotachophoresis assays†

G. V. Kaigala,[a] M. Bercovici,[b] M. Behnam,[c] D. Elliott,[c] J. G. Santiago[a] and C. J. Backhouse*[c]

Received 10th March 2010, Accepted 25th May 2010
DOI: 10.1039/c004120c

We present an inexpensive hand-held device (240 g) that implements microchip isotachophoresis (ITP) with laser induced fluorescence (LIF) detection. This self-contained instrument integrates the functionality required for high voltage generation onto a microelectronic chip, includes LIF detection and is powered by a universal serial bus (USB) link connected to a laptop computer. Using this device we demonstrate focusing and detection of a fluorescent species with a limit of detection of 100 pM. We show that the response of the detector is linear with the initial analyte concentration, making this device suitable for quantitative analysis. We also demonstrate the use of our simulation tools for design and prediction of ITP assays, and validate these results with a demonstration of multiplexed indirect detection of (unlabeled) analytes performed using the device. We find good agreement between simulations and experimental results. Using a label-free isotachaphoresis assay implemented in the hand-held device we detect two explosives and an endocrine disruptor spiked in river water, with no prior sample processing.

1. Introduction

Isotachophoresis (ITP) is an important tool in the field of analytical separations and detection.[1] ITP allows for simultaneous separation and concentration and is useful for lab-on-a-chip (LOC) systems as it offers high sensitivity[2] and adequate separation resolution even with order 1 cm channel lengths and moderate applied voltages (order 1 kV and below).[3,4] Bocek and co-workers recently reviewed the use of ITP in diverse applications including environmental monitoring, pharmaceuticals, food analysis, forensics, and chemical and biological detection.[1] Between the years 2004–2008, an average of more than one paper per week was published on ITP-related work.‡ Despite such diverse and widespread applications of ITP, on both traditional capillaries and microchips, the use of this technique has been limited to a laboratory setting as the necessary infrastructure is typically bulky, expensive and complex (*e.g.* power supply, microscope). The wider application of ITP outside a typical laboratory will require highly portable and cost-effective instrumentation.

In ITP, a sample mixture is introduced between leading and terminating electrolytes having respectively high and low effective electrophoretic mobilities. Under an applied electric field, co-ionic species focus and simultaneously separate into segregated zones according to their respective effective electrophoretic mobilities.[6] Common detection strategies in ITP are conductivity, UV absorbance, and direct fluorescence detection of analytes. While conductivity detection can be potentially easy to miniaturize, direct contact conductivity can result in fouling of electrodes, while contactless conductivity detection is typically limited by high limits of detection (LoD).[7] UV absorbance is not particularly suited for microchip implementations due to the common use of borosilicate glass (*versus* fused silica) and because most chips have fairly short optical path lengths which leads to low sensitivity.[8] Fluorescence is the most sensitive on-chip detection technique.[2,9] The signal in fluorescent detection can be maximized with minimum background by delivering spectrally precise excitation illumination, at the excitation peak of the fluorophore. Compared to light emitting diodes (LEDs), diode lasers deliver a relatively collimated illumination that is readily directed into micron size channels and has relatively narrow spectral width (*e.g.* several nm at full width half maximum). This makes laser induced fluorescence (LIF) detection a good choice for on-chip detection in ITP.

Several commercial bench-top (order 10's of kg) LIF-based microchip electrophoresis analysis systems are available, such as the Agilent 2100, BioRad's BioFocus/Experion, Caliper's LabChip 90 system and Hitachi's SV1100. Limited technical information is available about these systems. The Mathies group has shown several demonstrations[10,11] of portable systems and these along with that of Sandia National Laboratories,[12,13] exemplify the state of the art in high performance portable LIF-CE systems. However, as pointed out by Myers and Lee,[14] these systems are relatively expensive and significant effort is needed to further miniaturize, automate and to reduce costs, particularly of the optical modules.

In this work, we focus on the development and demonstration of a portable, yet low-cost ITP instrument. Key to this system is a compact and low-power implementation of a high voltage supply and a laser-induced fluorescence module. At the University of Alberta, we have been progressively shrinking LOC

[a]*Department of Mechanical Engineering, Stanford University, Stanford, CA, 94305, USA*
[b]*Department of Aeronautics and Astronautics, Stanford University, Stanford, CA, 94305, USA*
[c]*Department of Electrical and Computer Engineering, University of Alberta, 2nd Floor, ECERF, Edmonton, AB, T6G2V4, Canada. E-mail: chrisb@ualberta.ca; Fax: +1 780-492-1811*

† Electronic supplementary information (ESI) available: Details about the sub-components of the hand-held instrument. See DOI: 10.1039/c004120c

‡ Between the years 2004 to 2008, 331 publications resulted in the search topic "isotachophoresis," refined by the category "science and technology," and document type as "article" according to the ISI Web of Science search engine, www.isiknowledge.com/.

instrumentation while simultaneously incorporating components which are cost-effective and compatible with capillary electrophoresis (CE) systems with LIF detection. As an earlier prototype, Kaigala *et al.*[15] demonstrated a shoe-box sized system using EMCO (Sutter Creek, CA, USA) DC–DC converters to generate high voltage and a charge coupled device (CCD) camera as a detector to demonstrate the feasibility of an inexpensive non-confocal electrophoresis instrument. Subsequently, Behnam *et al.*[16] presented a high voltage module by the use of microelectronic technology and demonstrated a 3×4 mm (12 mm^2) HV CMOS chip which generates and switches up to 300 V from an input. Using this microelectronic chip and replacing the CCD camera with a photodiode, Kaigala *et al.*[17] demonstrated a compact system for direct detection of separated DNA. However, as there is a clear tradeoff between performance, compactness and cost, the system had a limit to detection of deoxyribonucleic acid (DNA) concentration 70 ng μL^{-1} (or $\sim$350 nM).

Here we present a higher performance and more compact version (cell phone sized) of the above instrument (Kaigala *et al.*[17]) which is adapted to an ITP. The system uses a low-cost photodiode and yet overcomes some of the earlier limitation[17] of low sensitivity by integrating ITP to increase the signal. The current authors have also reduced the noise in the detection circuitry both by improvements in the amplifier design, and by use of better shielding. Furthermore, we now make use of a low power microcontroller which performs time-critical functions within the device, without dependency on the interfaced computer. Using this new highly compact instrument, we demonstrate its versatility by implementing three ITP assays and detecting both cationic and anionic analytes. We demonstrate focusing and detection of small fluorescent species with a limit of detection (LoD) of 100 pM (to our knowledge, the first demonstration of ITP with direct fluorescence-based detection on a low-power hand-held device). This shows that ITP can be used to compensate for the losses in LoD incurred by the use of photodiodes and minimal optics. We further demonstrate the applicability of the device for indirect detection of unlabeled analytes using recent techniques developed by Chambers and Santiago[18] and Bercovici *et al.*[19] and also discuss the use of simulation tools for interpretation of results and design of assays for this device. Lastly, we demonstrate label-free detection of two water-soluble explosives and an endocrine disruptor spiked in river water, with no sample preparation steps.

2. System architecture

2.1 Miniaturized electrophoresis device design

Two key functional components of our hand-held instrument are the high voltage module, and the optical sub-system. Both components along with the microfluidic chip (see Section 2.3) are housed within a metal casing (dimensions $7.6 \times 5.7 \times 3.8$ cm and weight of 240 g with all components) which additionally acts as a Faraday cage to reduce noise pick-up by the sensitive optical electronic circuits. The instrument is autonomously controlled by the firmware (Section 2.2) resident within the microcontroller. The simple, standard metal casing we chose accounts for over 80% of the system weight. Also, we estimate the components take up only 40% of the inside volume of this casing. We therefore believe package design efforts can substantially decrease the size and weight of the system further.

HV functionality. HV generation in LOC systems is typically implemented using DC–DC converters together with mechanical relays which tend to be large, bulky and expensive (*e.g.* ref. 12,15, and 20). In previous work,[16] the University of Alberta group has integrated the HV generation and switching functionality into a single microelectronic chip. Briefly, this microelectronic chip generates high voltage using a non-isolated inductive DC–DC boost converter circuit.[21] It is fabricated using DALSA Semiconductor's (Bromont, QC, Canada) three metal layer, triple well, dual gate oxide 0.8 μm 5 V/HV CMOS/DMOS process. This microfabrication process technology supports the integration of both the HV components and low voltage components (for control, data communication) within a single die. The main (functional) subsystems of this microelectronic chip are (a) programmable HV generation module, (b) eight independently controlled HV switched-outputs that can be coupled to the microfluidic chip, and (c) an interface subsystem, which controls and monitors the microelectronic chip functionality and communicates to external devices using a standardized serial peripheral interface (SPI) protocol. Our device voltage and current were initially limited to 154 V and $\sim$30 μA. In the assays presented here, current was more than an order of magnitude lower than this limitation. Therefore, to minimize assay time, we operated at the maximum available voltage in all experiments presented here.

Optics sub-system. Commonly used components in LOC-based electrophoresis systems are confocal optics, dichroics, and detectors such as photomultiplier tubes (PMTs)[10,12] and CCDs,[15] which can be sensitive but typically expensive and bulky. For fluorescence detection we make use of a photodiode (NT57-506, Edmund Optics, Barrington, NJ 08007-1380 USA) having a responsivity of 0.4 A W^{-1} at 670 nm and an active area of 450×450 μm and which is connected to a high gain amplifier circuit (10^9 V A^{-1}).

To reduce the overall component cost of the device, we use minimal optics. The optics components we integrated consist simply a miniature lens and an interference filter. The entire optical detection module is housed in a barrel, and is placed at a fixed location below the microfluidic chip. The barrel consists of a compact (1.8 mm diameter and 5.37 mm long) gradient index (GRIN) microlens with a numerical aperture of 0.46 mm (LGI630-6, Irvine, CA, USA) for collection of the light emitted from the microchannel, and an interference filter (HQ660LP, Chroma Technology Corp., VT, USA) to minimize the excitation light detected by the photodiode. A compact 5 mW semiconductor laser diode with an excitation maximum at 635 nm (M635-5, US-Lasers, Inc., Baldwin Park, CA, USA) is used as the excitation light source. Much as in one of the configurations described in Fu *et al.*,[22] we illuminate the light through the edge of the chip in order to maximize the signal from the fluorophores within the microchannel, avoid direct incident light on the detector, and minimize scatter from the walls. This ensures a low baseline in the detected signal while increasing the dynamic range of the measurements. We initially observed slowly varying noise

in the detected signal which originated from laser intensity variations. We successfully minimized these variations by ensuring the thermal stability of the laser. This was accomplished by enhancing the thermal coupling between the laser, heatsink and the metal casing by using 3M™ thermal interface tape (3M, St Paul, MN, USA). Additionally, we performed warm-up periods in which the laser was left on for 5 min before each set of runs.

2.2 Control and data processing

The instrument consumes less than ~300 mW and this power is provided *via* the serial (USB) link connection to a laptop computer. The interfaced computer runs a custom graphical user interface program into which the user enters the parameters of the run (*e.g.* voltage and timing). These data are transferred to the firmware resident in the microcontroller, which directly controls both the high voltage module, and the optical module. A brief description of the firmware and the software is provided below, while detailed descriptions of similar architecture are described elsewhere.[23]

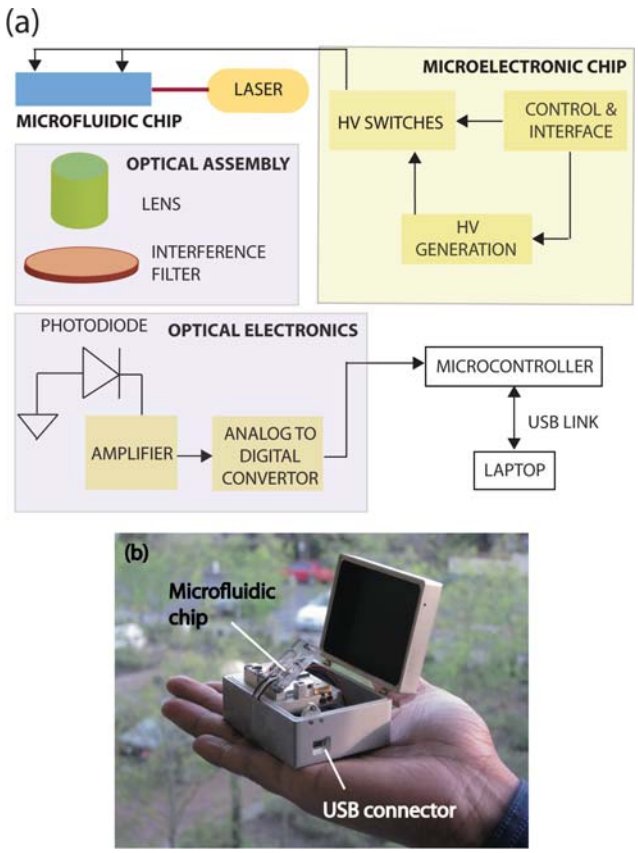

Fig. 1 (a) Functional block diagram of the individual modules within the hand-held device. This instrument consists primarily of a high voltage unit and a laser induced fluorescence detection system. More details are given in the ESI†. In (b), the hand-held ITP instrument (dimensions: 7.6 × 5.7 × 3.8 cm) is powered using a standard USB link connected to a laptop computer. The instrument is self-contained and includes a 5 mW laser, a photodiode, high voltage generation, switching, and communication functionality. The metal casing acts as a Faraday cage to reduce the effects of environment noise.

At the heart of the device is a microcontroller (PIC microcontroller, PIC 18F4550, Microchip Technology, Inc., Chandler, AZ, USA) serving as a real-time operating system. We implemented (in C language) multiple functionalities including initialization of each hardware module, communication protocols, control algorithms, and data acquisition. The microcontroller communicates with the external computer (*e.g.* a small laptop) *via* a USB serial link.

The controlling computer runs a Python script (open source, and portable between operating systems) which performs multiple functions including issuing the run parameters to the microcontroller, logging raw data, and performing data processing. Importantly, the Python code also presents a graphical user interface (GUI) in which the user can easily define the run-parameters. The data acquired by the detector, together with GUI parameters identifying the run, are recorded as a standard ascii file. At the end of each run, the Python script also creates an html report consisting of a header detailing the run parameters and two embedded.png images showing signal *versus* time plots of raw and signal-processed data.

While the GUI can perform the required signal processing of the raw data, for this study we performed the processing using Matlab (R2007b, The Mathworks, Natick, MA, USA). We remove the high frequency noise by convolving the raw data with a Gaussian whose width (one standard deviation) equals to the residence time of the edge of an ITP zone over the GRIN lens (Fig. 1). This preserves the underlying fluorescence signal from the ITP zones while increasing signal-to-noise ratio (SNR).

2.3 Microfluidic chip

We perform the experiments using custom-built microfluidic chips (~2 cm × 1.5 cm). Each chip contains a single cross-channel design suitable for both finite injection (not used within this work), and infinite sample injection (described here). The injection scheme and assays described here can therefore be accomplished with a simple one channel, two reservoir system.

The chip consists of two layers of borofloat glass (Paragon Optical Company, Reading, PA, USA) each 1.1 mm thick. The bottom layer contains the etched channels, while the top layer contains Waterjet system (Bengal, Flow International Corp., Kent, WA, USA) drilled 2 mm diameter holes which serve as reservoirs. Each of the four reservoirs holds up to about 4 μL of reagents. The chip was fabricated using a standard microfabrication procedure. Briefly, the channel geometry was drawn in L-Edit v3.0 (MEMS Pro 8, MEMS CAP, CA, USA) and transferred to a mask wafer using a pattern generator (DWL 200, Heidelberg Instruments, Torrance, CA, USA). The 4″ × 4″ glass was cleaned in hot Piranha (3 : 1 of H_2S0_4 : H_2O_2) and sputter-coated with 30 μm of Cr and 180 μm of Au. HPR 504 photoresist (Fujifilm USA Inc., Valhalla, NY, USA) was spin coated (spin speed of 500 rpm for 10 s and a spread speed of 4000 rpm for 40 s). The substrates with photoresist were then baked in an oven at 115 °C for 30 min. UV exposure (4 s, 356 nm and with intensity of 19.2 mW cm^{-2}) of the spin-coated substrate was performed through the mask using a mask aligner (ABM Inc., San Jose, CA, USA) and then the substrate was chemically developed with Microposit 354 developer (Shipley Company Inc., Marlborough, MA, USA) for ~25 s. Glass was etched at ~1 μm min^{-1} using

hydrofluoric acid (20 : 14 : 66 HF (49%) : HNO_3 (70%) : H_2O). The substrate was then etched to a depth of 10 μm. Then, Au etch (0.0985 M I_2 + 0.6024 M KI) and Cr etch (Arch Chemicals Inc., Norwalk, CT, USA) were used to strip the metal (~45 s for Au and ~30 s for Cr). Holes in the top layer for accessing channels in the assembled chip were drilled using a Waterjet. The two glass layers were mated to form the complete chip, heated in an oven for ~4 h at 550 °C, and diced to form the individual chips (Fig. 2a).

3. Experimental setup and assay descriptions

In Section 3.1 we present the setup for direct detection of a fluorescent dye. In Section 3.2 we present indirect detection of multiple analytes. In the latter, the electromigration rate and the length of analyte zones are strongly coupled and we show that our numerical simulation tool can predict this coupling and can be used for design and the (non-trivial) interpretation of assays operated under constant voltage. All experiments in this paper (with the exception of the data presented in Fig. 7) were performed with 154 V of constant voltage using the custom-made chip shown in Fig. 2. During the course of this work, we improved the performance of the high voltage sub-system and generated 204 V of constant voltage, and this voltage is used for the results presented in Fig. 7. We make use of a semi-infinite injection protocol (as detailed in Section 3.1) and for this use only the segment of the channel between reservoir 1 and 4 (channel length 28 mm and a nominal electric field 55 V cm^{-1}) for direct detection and segment of channel between reservoir 2 and 4 (channel length 23 mm and a nominal electric field 66.6 V cm^{-1}) for indirect detection. When the chip is placed within the hand-held device for analysis (Fig. 1), the photodetector is located 8 mm from reservoir 4.

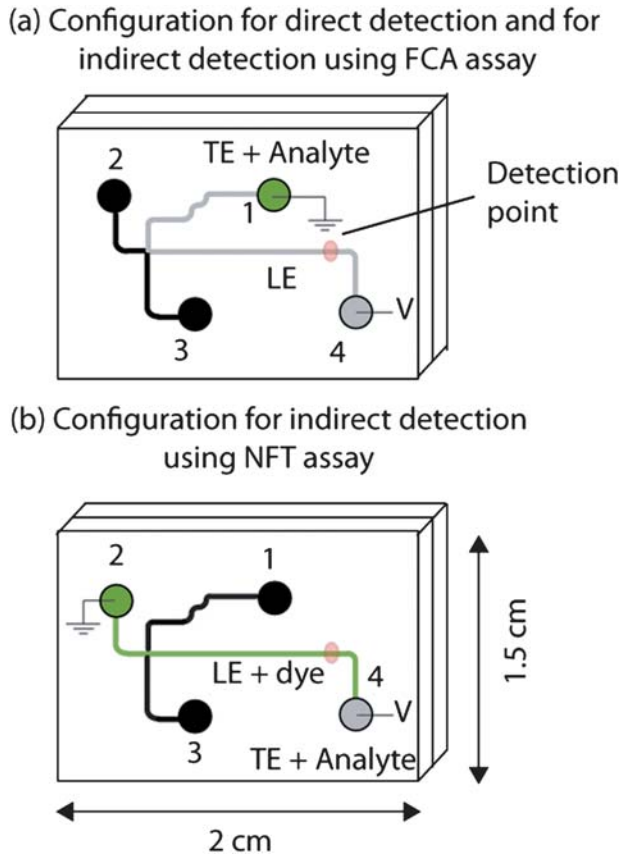

Fig. 2 ITP is conducted in a custom-fabricated microfluidic chip (~2 cm × 1.5 cm) wherein micro-sized (10 μm deep and 30 μm wide) channels are isotropically etched in a 1.1 mm thick borofloat glass. A second, 1.1 mm thick borofloat glass is drilled with through-holes and two layers are bonded using a standard low-temperature glass–glass bonding procedure. When the chip is placed within the hand-held device, the detection point is located ~8 mm from reservoir 4. Using this chip, we perform both direct detection of analytes with channels and reservoir filled as shown in (a), and indirect detection of analytes using non-focusing tracer (NFT) assay with channels and reservoir filled as shown in (b) (operation described in Section 3). The fluorescent carrier ampholyte (FCA) assay is implemented on an identical microfluidic chip but with varying etch depths channels, the larger cross-section is 55 μm wide, 25 μm deep, and 11 mm long (starting from reservoir 1). The small cross-section is 15 μm, 5 μm deep, and 17 mm long wide (starting from reservoir 4). The variable etching time affects both the width and the depth of the channel and results in a 17 : 1 cross-sectional ratio.

3.1 Direct detection ITP assay

In ITP, sample ions are focused between a high electrophoretic mobility leading electrolyte (LE) and a low electrophoretic mobility trailing electrolyte (TE). In the injection scheme we implemented here (semi-infinite sample injection), the sample is mixed in the TE reservoir while the rest of the channel is initially filled with LE (Fig. 3a). Under an applied electric field, sample ions with a higher electrophoretic mobility than TE ions (the TE is chosen to guarantee this) overspeed the TE and accumulate (focus) at the LE–TE interface, since they cannot overspeed the high mobility LE. This leads to a narrow region of increased analyte concentration (also known as "peak mode" ITP), which electromigrates in the channel while continuously accumulating additional sample (Fig. 3b). For fluorescent samples (either

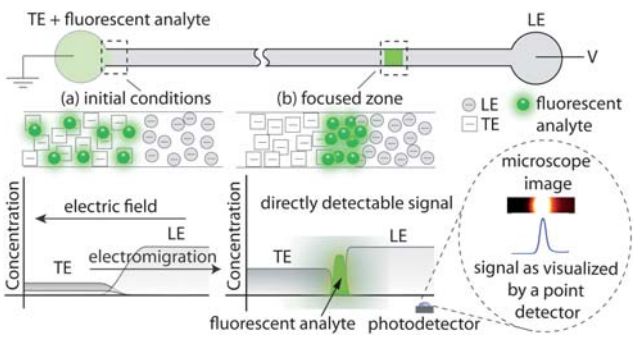

Fig. 3 Schematic of "peak-mode" isotachophoresis with single-interface injection. A microchannel is connected to two reservoirs, with the analyte mixed in the TE reservoir as shown in (a). When an electric field is applied along the channel all ions in the system migrate according to their effective electrophoretic mobility and local electric field. Since the LE and TE mobilities are chosen to bracket that of the analyte, the analyte focuses at the LE/TE interface as seen in (b). A fluorescent analyte initially forms a Gaussian-like peak as shown. The detail view at the bottom right shows an actual CCD camera image of a peak mode ITP zone. Beneath this, is a simulated point detector signal obtained by convolving the spatial image with an ideal point detector represented by a delta function.

labeled or autofluorescent), the increased concentration translates directly to an increase in fluorescence intensity which can be detected by a photodetector further along the channel. Multiple analytes, if bracketed by the LE and TE mobilities, will focus at the LE/TE interface, and will appear as a single zone (assuming all the species are fluorescent at the same wavelength). For this reason, direct detection in peak mode can typically only be achieved using highly specific labels which bind only to a specific analyte of interest. If multiple analytes are present, then it is possible to introduce non-fluorescent spacer ions to separate the focused species.[3]

Buffers for direct detection ITP. For this anionic ITP, the LE was composed of 250 mM HCl and 500 mM bis-tris and the TE was 5 mM tricine and 10 mM bis-tris. A range of Alexa Fluor 647 from 100 pM to 2 nM (Invitrogen, Carlsbad, CA, USA) were added to the TE as sample. The LE and TE each contained 1% of ~1 MDa poly(vinylpyrrolidone) (PVP) for suppression of electroosmotic flow (EOF). All buffers were prepared in deionized water (UltraPure DNase/RNase free distilled water, GIBCO Invitrogen, Carlsbad, CA, USA) and prepared using chemicals obtained from Sigma Aldrich (St Louis, MO, USA) unless otherwise specified.

Chip cleaning, filling, and insertion procedure. Before each set of runs we cleaned the channels by flowing NaOH for approximately 5 min, and then rinsed the channels with deionized water for 2 min. We then flushed the channels with LE solution for 5 more min to allow the PVP to coat the walls. For the direct detection experiments we filled reservoirs 1, 2 and 3 of the chip with 4 μL LE and applied a vacuum at reservoir 4 until all channels were filled (~2 min). We then rinsed reservoir 1 several times with distilled water (using a syringe) and then filled it with the TE and analyte mixture. The chip was then placed in position within the hand-held device, and the system's chip latch (a small hinged acrylic cover which holds electrodes and the chip in place) was lowered into a position wherein platinum electrodes were inserted into the buffers in reservoirs 1 and 4.

3.2 Indirect detection ITP assays

Two indirect detection techniques based on ITP were recently developed by Chambers and Santiago[18] and Bercovici *et al.*[19] Both techniques are based on "plateau mode"[6] ITP. Analytes initially focus in peak mode as described earlier. An analyte with sufficient solubility continues to accumulate and reaches a limiting concentration. This limiting concentration value is determined by LE chemistry and analyte properties.[6] In this plateau mode, additional sample accumulates and increases the length of each analyte zone. Further, plateau-mode analyte zones clearly self-segregate according to their effective electrophoretic mobilities. The result is purified adjacent zones as shown in Fig. 4. This example shows a schematic for the case of three separated and focused analytes in plateau mode. The concentration of analytes is locally uniform within each analyte plateau region. The conductivity varies from zone to zone (monotonically decreases from LE to TE), and this results in changes in the local electric field (electric field accordingly increases monotonically from LE to TE). The zones are visualized using the non-focusing tracer and fluorescent carrier ampholyte assays, as described below.

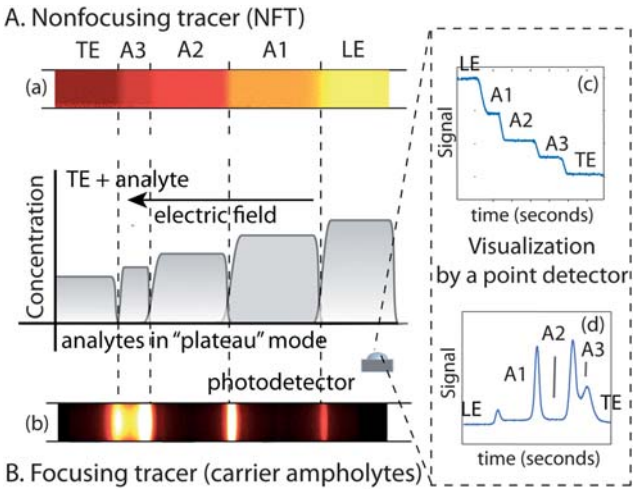

Fig. 4 Schematic of non-focusing tracer (NFT) and fluorescent carrier ampholyte (FCA) techniques for quantitative indirect detection of multiple analytes using plateau mode isotachophoresis. Under an applied electric field, analytes simultaneously focus and separate according to their effective electrophoretic mobilities. After sufficiently long separation distance and sufficiently high initial analyte concentration, distinct analyte zones with locally uniform concentrations are created (denoted here in the center plot as analytes A1, A2, and A3). In NFT (a) the unlabeled analytes are detected by introducing a single fluorescent counterion which electromigrates through the ITP zones, adjusting its concentration to the local electric field. A point detector located downstream captures a step in the fluorescence signal for each new analyte zone (c). In FCA (b) analytes simultaneously focus with a mixture of a relatively large number of fluorescently labeled carrier ampholytes and displace subsets of carrier ampholytes creating detectable and specific gaps in the fluorescent signal (d). The two schematic plots in the inset represent data obtained by a convolution of the spatial signals with an ideal point detector represented by a delta function.

The indirect detection technique developed by Chambers and Santiago[18] is termed the non-focusing tracer (NFT) assay. In one of its variations, it makes use of a low concentration counterionic fluorophore (tracer) mixed in the LE reservoir. Under an applied electric field, the tracer electromigrates in the opposite direction to ITP. As the tracer enters each zone, its concentration adapts to the local electric field, as dictated by the conservations of current and species. Fig. 4 presents an actual microscope image of the fluorescent signal resulting from the detection of three (non-fluorescent) analytes. The NFT clearly delineates the plateau zones of each analyte. When captured by a downstream point detector the signal shows multiple "steps" in the fluorescence signal, each indicating an interface between different zones. Fig. 4c shows a schematic of data as visualized by a point detector for the same conditions and analytes of the experiment in the image.

The second indirect detection technique implemented here was developed by Bercovici *et al.*[19] and is termed as fluorescent carrier ampholyte (FCA) assay. In this technique, the background fluorescence signal is created using low concentrations of fluorescently tagged carrier ampholytes (CAs) added to the trailing electrolyte. In the absence of analytes, tagged carrier

ampholytes form a continuous fluorescent zone in the channel. An analyte focuses within this CAs train at a highly specific location determined by its effective mobility. In doing so, it displaces a subset of the CAs creating a gap (or "valley") in the fluorescent signal (Fig. 4b and d). As discussed by Bercovici *et al.*[24] the assay allows detection of unknown toxins with no prior knowledge of their electrophoretic properties. Furthermore, no pre-treatment of the water sample is required.

In plateau mode ITP, limit of detection (LoD) is the minimum initial concentration of the analyte at which a zone can be detected. For a given analyte concentration, increasing the length of the zone is equivalent to improving the LoD. Longer zone lengths can be achieved by choosing appropriate ITP buffers and optimized microchannel geometries. An important complication of running experiments at constant voltage is that analyte zones then affect substantially the resistance of the channel and hence the instantaneous electromigration velocity. In Section 4.2 we will present results obtained under constant voltage, and provide a comparison with numerical results.

Buffers for indirect detection using NFT. For this cationic ITP, the LE was 10 mM NaOH and 20 mM BES (*N*,*N*-bis(2-hydroxyethyl)-2-aminoethanesulfonic acid). 40 μM of Alexa Fluor 647 (Invitrogen, Carlsbad, CA, USA) were mixed in the LE to serve as a counterionic non-focusing tracer. The TE consisted of 2.5 mM pyridine and 5 mM BES. 500 μM each of bis-tris(bis(2-hydroxyethyl)-amino-tris(hydroxymethyl)-methane), tris(tris(hydroxymethyl)aminomethane), and histidine were added to the TE as analytes. Both the LE and TE contained 1% of ~1 MDa poly(vinylpyrrolidone) (PVP) for suppression of electroosmotic flow (EOF).

Buffers for indirect detection using FCA. For this anionic ITP, the LE was 10 mM hydrochloric acid and the counterion is 20 μM bis-tris. The LE reservoir is titrated to a pH of 6.9 with 5 μM of NaOH. The TE is 10 mM tricine and the counterion is 20 μM bis-tris. 1 μM of ZOOM 3–10 labeled with Alexa Fluor 647 was mixed in the TE. Both the LE and TE contained 1% of ~1 MDa poly(vinylpyrrolidone) (PVP) for suppression of electroosmotic flow (EOF). For these experiments demonstrating the detection of explosives and herbicides, we prepared stock solution of 100 μM ammonium 2,4,6-trinitrophenolate (Dunnite) and 2,4,6-trinitrophenol (TNP) and dichlorophenoxyacetic acid (2,4-D). These analytes were diluted into a TE/sample mixture that had a final composition of 50% river water. The river water was collected from Vernal Falls, Merced River, Yosemite Valley, CA, USA (conductivity measured as 25 μS).

Chip filling procedure. For the FCA implementation, the chip filling procedure is identical to as outlined in Section 3.1. For the NFT implementation we used a similar procedure, except reservoirs 1, 3 and 4 were originally filled with LE, and TE was introduced in reservoir 2.

4. Results

A large number of ITP protocols can be implemented on this hand-held instrument. We here choose to implement two representative ITP protocols. The first of these demonstrates direct detection of a fluorescent analyte in peak mode ITP. The second protocol demonstrates indirect fluorescence-based detection of non-fluorescent analytes in plateau mode ITP.

4.1 Focusing and direct detection of fluorescent species

We first demonstrate direct detection of an idealized analyte, Alexa Fluor 647 (an anionic fluorophore), on the hand-held device (Fig. 1). We varied the initial concentration of sample in the reservoir, and registered the fluorescence signal as detected by the photodetector. The inset in Fig. 4 shows four typical signals obtained for initial concentrations of 0.1, 0.5, 1, and 2 nM. The main plot presents a quantitative measure of the maximum signal intensity *versus* the initial concentration of the dye. The uncertainty bars represent 95% confidence on the mean based on five realizations at each concentration, and the curve is a linear best fit using the mean values. The linear response between initial analyte concentration and the signal detected suggests that ITP implemented on this hand-held instrument is suitable for quantitative analysis. In peak mode ITP, we define the limit of detection (LoD) to be the lowest initial sample concentration resulting in a signal-to-noise ratio (SNR) of 3 (with SNR here defined as the ratio of peak magnitude to the standard deviation of the variation in the baseline established from the first 30 s prior to the arrival of the LE-dye interface). For the ITP protocol we present here, we find the LoD to be 100 pM (five repetitions were performed, see Fig. 5).

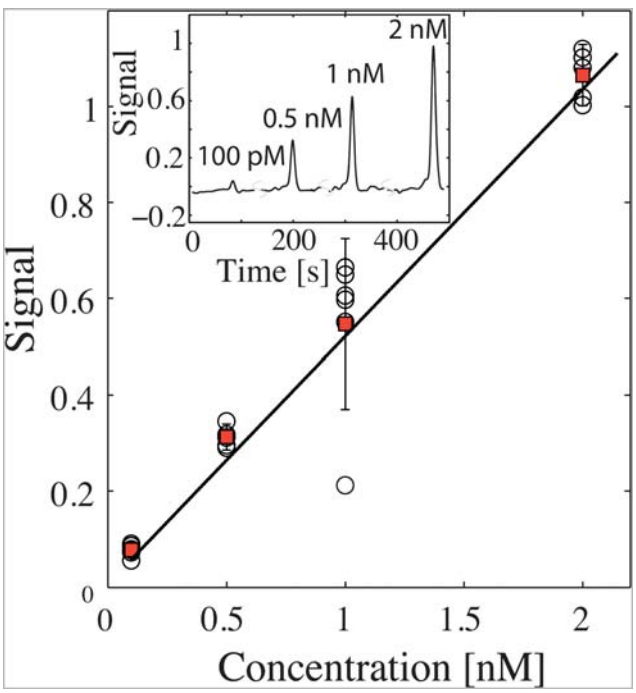

Fig. 5 Focusing and direct detection of a fluorescent species (Alexa Fluor 647) using "peak mode" ITP in our portable device. The response of the detector was linear with the initial concentration of the analyte. Five repetitions were performed at each analyte concentration. The uncertainly bars represent a 95% confidence interval on the mean value, based on the Student *t* distribution. The inset shows a superposition of actual signal data registered by the hand-held device for four initial concentrations.

We attribute the mostly minor variability in signal intensity (see Fig. 5) for fixed initial concentrations to run-to-run variations associated with both the instrument and the assay. Signal variations arising from the instrument are likely the result of loose tolerances in positioning of the chip on the device, which leads to slight variations in the amount of light coupled into the channel. We hypothesize that variations arising from the assay are due to manual pipetting uncertainties and run-to-run variations in EOF (despite our efforts to suppress EOF). The system/instrument related variability can likely be reduced with improved mechanical design, and the variability in EOF can perhaps be addressed with improved surface passivation. We are presently pursuing both approaches to reduce this run-to-run variability.

4.2 Indirect detection of multiple analytes

We here demonstrate the use of our (free and open source) simulation tool[25] (Spresso) in the design and prediction of an indirect detection assay for detection of cationic analytes. Using a set of experiments on our hand-held device we validate the simulations and exhibit the device's ability to provide quantitative multiplexed indirect detection. Comparison between the simulations and data also reveals important considerations in interpreting ITP measurements obtained with limited and constant applied voltage.

Fig. 6a presents a sequence of simulations wherein we detect unlabeled tris, histidine, and bis-tris using a non-focusing tracer (Alexa Fluor 647) mixed in the LE. We used 200 grid points in the simulation, over a 33 mm long computational domain. The simulations were performed in a stationary frame of reference, with 154 V applied across 23.1 mm (the total length between reservoir 2 and 4). We used the nominal electrophoretic mobilities and dissociation constants given by Hirokawa *et al.*[26] and a pre-determined electroosmotic wall mobility (the choice of this value is further described below). The concentrations of all analytes in the domain were saved at each time step, and we used a separate Matlab code to calculate the concentration of the tracer *versus* time (emulating a point detector). Fig. 6a(I) presents a negative control case, where we see a single step in the signal, corresponding to the interface between the LE and TE. In (II) we added bis-tris to the TE reservoir. Bis-tris focused and created a new zone between the LE and TE. In (III) we add tris (in addition to bis-tris). Tris has a higher electrophoretic mobility and therefore focused in front of bis-tris (detected at an earlier time). Similarly, addition of histidine (which has a lower effective mobility than bis-tris) Fig. 6a(IV) resulted in a new zone trailing bis-tris.

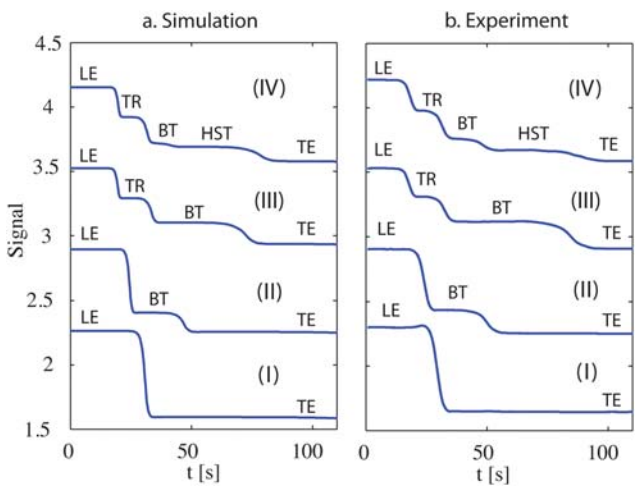

Fig. 6 Demonstration of separation and NFT-based indirect detection of three model analytes using the hand-held device. The left-hand column (a) presents simulation results (using Spresso[25]) with conditions identical to those of experimental results in the right-hand column (b). In the control (I), a single 'step' appeared, corresponding to the interface between the LE and TE. When 500 μM bis-tris (BT) was mixed with the TE (II), an additional zone appeared between the LE and TE. The addition of tris (TR) (III) and histidine (HST) (IV) was also detectable as new zones appear in the signal. However, the addition of new analytes changed the length of previously detected zones. This strong coupling between the presence of analytes and temporal signal widths is due to the coupling between analyte conductivity and local electric fields, and was well captured in the simulation.

Fig. 6b presents results of a sequence of experiments performed on the hand-held device at conditions identical to those used in the simulations. We used an initial control experiment, Fig. 6b(I), to establish two parameters in our simulations. First, we accounted for residual electroosmotic flow (EOF) in the system (although largely suppressed using PVP). To this end, we set the electroosmotic wall mobility in the simulation so that the detection time of the LE–TE interface in the simulation matched with that of the experiment (this yielded a relative low value of 3×10^{-9} m^2 V s^{-1}). In the rest of the simulated cases (with analytes) we used this same (single) EOF value. Second, the signal in the experiment corresponded to measured fluorescence intensity, while simulation results provided directly all ion concentration values. We therefore scaled the y-axis of our simulation results so that the step height in the control case matched with the experiment and subsequently used the same scaling for the rest of the simulations. With just these two parameters established using a control experiment, we find good agreement between the computational and experimental results in both the lengths and relative signal intensities of analyte zones.

We note that while the initial concentration of bis-tris was the same for cases (II) and (III), the temporal width (the width of the zone along the time axis) of its zone was much larger when tris was present (III). This is due to the constant voltage scheme we employed which, while minimizing assay time, resulted in strong coupling between electromigration velocity and the analyte zones. For example, at the time when the bis-tris zone first arrived at the detector, the electromigration velocity was lower in case (III) (bis-tris and tris) than in case (II) (bis-tris alone). This was because the presence of tris (rather than just LE) increased the resistance of the channel, resulting in lower electric field in the LE and lower ITP velocity. As a result, the bis-tris zone took significantly longer time to cross the detector. Similarly, when histidine (which focused behind the bis-tris zone) was added in case (IV), the temporal width of the bis-tris zone was again smaller. This was because the histidine zone had a higher conductivity than the TE zone, and the channel therefore had an overall lower resistance (and a higher ITP velocity) when bis-tris reached the detector.

This experimental validation demonstrates the ability to design and interpret indirect ITP assays for multiplexed detection on the hand-held device, using a limited maximum voltage.

4.3 Indirect detection of explosives and endocrine disruptor in river water

We applied our hand-held device to detect indirectly (label-free) ionic water soluble explosives, ammonium 2,4,6-trinitrophenolate (Dunnite) and 2,4,6-trinitrophenol (TNP), and a herbicide, dichlorophenoxyacetic acid (2,4-D). 2,4-D is the world's most common herbicide (third-most common in the US) and has, importantly, been implicated as an endocrine disruptor in potable water. Detection of explosives in the environment plays an important role in warfare, and few techniques exist for detecting highly polar and ionic explosives and their degradation products[27] We spiked the samples in river water (Vernal Falls, Merced River, Yosemite Valley, CA, USA) and focused, separated, and detected with no additional sample preparation. Fig. 7a shows a control run performed using river water with no added analytes. Fig. 7b–d, respectively, show the detection of 50 μM Dunnite, 50 μM TNP, and 50 μM 2,4-D, spiked in the river water. Each of the analytes focuses at a highly specific location determined by its effective mobility, displacing a subset of the CAs and creating a gap (or "valley") in the fluorescent signal. The amount of displaced carrier ampholytes can be used for identification of an analyte.[24] In the figure, we indicate the value of the normalized signal integral (NSI) which, as described by Bercovici *et al.*,[24] can be used to analyze and identify chemical species. As shown by Khurana and Santiago,[3] the gap length is proportional to the initial concentration of the analyte. The limit of the detection corresponds to the lowest concentration for which a gap is still detectable. Based on Fig. 7, we conclude the LoD of our indirect detection is approximately 10 μM.

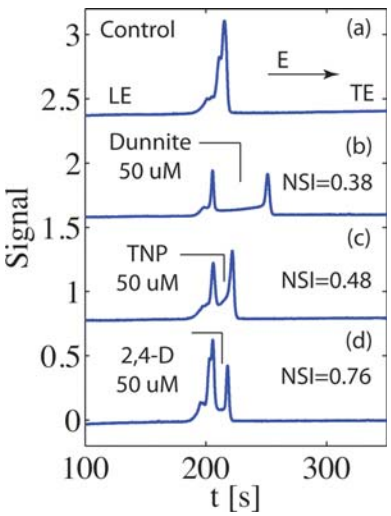

Fig. 7 Demonstration of indirect detection of explosives and an endocrine disruptor in river water, with no sample preparation steps. The signal in (a) shows a negative control (no analytes present). The fluorescent ampholytes form a contiguous (yet non-uniform signal). (b) 50 μM of ammonium 2,4,6-trinitrophenolate (Dunnite) were added to the TE reservoir. The analyte displaces a subset of the fluorophores and creates a detectable gap in the signal. (c and d) Indirect detection of 2,4,6-trinitrophenol (TNP) and 2,4-dichlorophenoxyacetic acid (2,4-D) respectively. LE is 10 mM hydrochloric acid, TE is 10 μM tricine and the counterion is 20 mM bis-tris. The LE reservoir was titrated to a pH of 6.9 with 5 μM of NaOH. 1 μM of ZOOM 3–10 labeled with Alexa Fluor 647 was mixed in the TE. 204 V was applied along a 23 mm channel with a 17 : 1 cross-section area reduction positioned 48% of the way long its length from the TE reservoir (the detection region is 17 mm from the channel inlet where samples are introduced). The baseline of each experiment was determined and subsequently subtracted from the signal using the GIFTS auto-leveling method using a fourth order polynomial with a 1% tolerance. For each detected analyte we also provide the normalized signal integral (NSI) value at the minima of the corresponding gap in signal. These values indicate the fraction of undisplaced fluorophores, and as discussed by Bercovici *et al.*,[24] can be related to the effective mobility of the analyte.

5. Concluding remarks

We presented a hand-held device for isotachophoresis, and demonstrated its practical application for three different isotachophoresis assays which use both direct and indirect detection of analytes. For direct detection, we showed that the device can provide quantitative analysis of fluorescent species, with a limit of detection of 100 pM. The sensitivity of the direct detection implemented on the hand-held device is adequate for several applications.[5]

For indirect detection, we demonstrated simultaneous detection of multiple analytes and showed that experiments can be designed and interpreted using our simulation tool. We have further demonstrated the use of the device for label-free detection of two explosives and an endocrine disruptor in unprocessed river water. We believe many applications, including water quality assessment and point-of-care disease diagnostics can benefit from a low-cost analysis system such as the one we presented here. We estimate our limit of indirect detection to be ~10 μM. Further by applying an LE concentration cascade[28] we believe an additional 10× increase in the LoD is possible. Thus an LoD of ~1 μM is already relevant for several applications (*e.g.* EPA permissible concentration of 2-chlorophenol, 2,4-dichlorophenol, and 2,4-dimethylphenol is ~1 μM), however for the detection of a wider range of explosives and herbicides (for 2,4-D about 300 nM[29]) in drinking water, further improvements are required. We are currently working to further reduce the limit of detection by optimizing the microfluidic channel geometry, together with improvements to optics and electronics hardware.

By leveraging the focusing ability in ITP we are able to utilize a low-cost and portable device yet achieve useful LoDs, thus overcoming many of the traditional trade-offs between cost and performance. The current total component cost of the hand-held device is ~$200, and we believe that with high volume production, cost of the instrument can be further reduced significantly. The device volume can be readily reduced ~50% by eliminating dead volume designed to allow easy access to components during the development stage. A lighter casing can be used to reduce weight by 50% or more. To our knowledge, this is the first demonstration of fluorescence-based ITP detection on a hand-held (7.6 × 5.7 × 3.8 cm, 240 g) and inexpensive device.

Acknowledgements

G.V.K. is supported by a postdoctoral fellowship from the Natural Science and Engineering Research Council (NSERC), Canada. M.B. is supported by an Office of Technology Licensing Stanford Graduate Fellowship and a Fulbright Fellowship. C.J.B. and D.E. acknowledge funding from NSERC. J.G.S. also gratefully acknowledge the support of the Defence Advanced Research Projects Agency contract number N66001-09-1-2007 (program manager Dr Dennis Polla) and for support from the Micro/Nano Fluidics Fundamentals Focus (MF3) Center funded by Defense Advanced Research Projects Agency (DARPA) MTO Grant No. HR0011-06-1-0050 and contributions from MF3 corporate members.

References

1 P. Gebauer, Z. Mala and P. Bocek, *Electrophoresis*, 2007, **28**, 26–32.
2 B. G. Jung, Y. G. Zhu and J. G. Santiago, *Anal. Chem.*, 2007, **79**, 345–349.
3 T. K. Khurana and J. G. Santiago, *Anal. Chem.*, 2008, **80**, 279–286.
4 W. N. Vreeland, S. J. Williams, A. E. Barron and A. P. Sassi, *Anal. Chem.*, 2003, **75**, 3059–3065.
5 L. Chen, J. E. Prest, P. R. Fielden, N. J. Goddard, A. Manza and P. J. R. Day, *Lab Chip*, 2006, **6**, 474–487.
6 F. M. Everaerts, J. L. Beckers and T. P. Verheggen, *Isotachophoresis: Theory, Instrumentation, and Applications*, Elsevier Scientific Publishing Company, Amsterdam, The Netherlands, 1976.
7 J. P. Landers, *Handbook of Capillary and Microchip Electrophoresis and Associated Microtechniques*, Taylor & Francis Group, LLC, Boca Raton, FL, USA, 2008, ch. 7.
8 S. Gotz and U. Karst, *Anal. Bioanal. Chem.*, 2007, **387**, 183–192.
9 M. E. Johnson and J. P. Landers, *Electrophoresis*, 2004, **25**, 3513–3527.
10 E. T. Lagally, J. R. Scherer, R. G. Blazej, N. M. Toriello, B. A. Diep, M. Ramchandani, G. F. Sensabaugh, L. W. Riley and R. A. Mathies, *Anal. Chem.*, 2004, **76**, 3162–3170.
11 P. Liu, T. S. Seo, N. Beyor, K. J. Shin, J. R. Scherer and R. A. Mathies, *Anal. Chem.*, 2007, **79**, 1881–1889.
12 R. F. Renzi, J. Stamps, B. A. Horn, S. Ferko, V. A. VabderNoot, J. A. A. West, R. Crocker, B. Wiedenman, D. Yee and J. A. Fruetel, *Anal. Chem.*, 2005, **77**, 435–441.
13 R. J. Meagher, A. V. Hatch, R. F. Renzi and A. K. Singh, *Lab Chip*, 2008, **8**, 2046–2053.
14 F. B. Myers and L. P. Lee, *Lab Chip*, 2008, **8**, 2015–2031.
15 G. V. Kaigala, V. N. Hoang, A. Stickel, J. Lauzon, D. Manage, L. M. Pilarski and C. J. Backhouse, *Analyst*, 2008, **133**, 331–338.
16 M. Behnam, G. V. Kaigala, M. Khorasani, P. Marshall, C. J. Backhouse and D. G. Elliott, *Lab Chip*, 2008, **8**, 1524–1529.
17 G. V. Kaigala, M. Behnam, C. Bliss, M. Khorasani, S. Ho, D. G. Elliott and C. J. Backhouse, *IET Nanobiotechnol.*, 2009, **3**, 1–7.
18 R. D. Chambers and J. G. Santiago, *Anal. Chem.*, 2009, **81**, 3022–3028.
19 M. Bercovici, G. V. Kaigala, C. J. Backhouse and J. G. Santiago, *Anal. Chem.*, 2010, **82**, 1858–1866.
20 E. T. Lagally and R. A. Mathies, *J. Phys. D: Appl. Phys.*, 2004, **37**, R245–R261.
21 N. Mohan, T. M. Undeland and W. P. Robbins, *Power electronics converters, Applications, and Design*, John Wiley and Sons, Inc., Hoboken, New Jersey, USA, 2003.
22 J. Fu, Q. Fang, T. Zhang, X. Jin and Z. Fang, *Anal. Chem.*, 2006, **78**, 3827–3834.
23 G. V. Kaigala, M. Behnam, A. C. E. Bidulock, C. Bargen, R. W. Johnstone, D. G. Elliott and C. J. Backhouse, *Analyst*, 2010, DOI: 10.1039/b925111a.
24 M. Bercovici, G. V. Kaigala and J. G. Santiago, *Anal. Chem.*, 2010, **5**, 2134–2138.
25 M. Bercovici, S. K. Lele and J. G. Santiago, *J. Chromatogr., A*, 2009, **1216**, 1008–1018.
26 T. Hirokawa, M. Nishino and Y. Kiso, *J. Chromatogr.*, 1982, **252**, 49–65.
27 M. Godejohann, A. Preiss, K. Levsen and G. Wunsch, *Chromatographia*, 1996, **43**, 612–618.
28 P. Bocek, M. Deml and J. Janak, *J. Chromatogr.*, 1978, **156**, 323–326.
29 Drinking Water Contaminants, US Environmental Protection Agency, http://www.epa.gov/ogwdw000/contaminants/basicinformation/2-4-d-2-4-dichlorophenoxyacetic-acid.html#four, 2010.

